Synthesis of hierarchically mesoporous anatase spheres and their application in lithium batteries†

Yu-Guo Guo, Yong-Sheng Hu* and Joachim Maier

Received (in Cambridge, UK) 10th April 2006, Accepted 10th May 2006
First published as an Advance Article on the web 25th May 2006
DOI: 10.1039/b605090e

Hierarchically mesoporous TiO_2 (anatase) sub-micron spheres with uniform particle size exhibiting high Li storage capacity and good cycling performance have been successfully prepared in a large quantity by using TiO_2–$CdSO_4$ composite as intermediate.

In recent years, nanoporous architectures with pore sizes ranging from one to hundreds of nanometers have been of considerable interest because of both fundamental science involved and technical applications targeted. The latter address catalysts, gas separators, sensors, and electrochemical energy converters.[1–4] Most of the nanoporous structures, which have thus far been considered, are prepared mainly *via* template-based methods, including soft templates (surfactants, chelating agents, block polymers, *etc.*)[5–7] and hard templates (porous anionic alumina, porous silica, polystyrene spheres, carbon nanotubes, *etc.*),[8–10] and usually contain periodically ordered micropores (<2 nm), mesopores (2 nm ~ 10 nm) and/or macropores (>50 nm). Considering ion insertion materials, which are important for electrochemical storage devices (*e.g.*, lithium batteries), there has always been a need for developing highly porous materials with large surface areas readily accessible to electrolyte, which, as a result, reduce the transport lengths for both electronic and ionic transport and improve the rate capability (*i.e.* the power density of a lithium battery).[11] The transport of small molecules in media featuring macropores plus large mesopores can approach rates of diffusion comparable to those in open medium,[12] which make these kinds of pore structures an important issue to be addressed in the context of lithium batteries. The small micropores are in the best case unimportant, since diffusion of molecules within microporous channels (<2 nm), such as those found in zeolites, typically exhibit hindered transport.[12] Also, the pore arrangement (*e.g.*, periodicity) is of minor importance with respect to transport as long as the network is percolating.[12] This is why, in this context, more emphasis should be laid on synthesis of optimized pore sizes and connectivity rather than striving for micropores or ordered arrangements. Here, we report on a novel facile synthesis of hierarchically mesoporous TiO_2 sub-micron spheres with high porosity and various large pores (3 nm ~ 50 nm). In addition, we demonstrate that these TiO_2 spheres are promising anode materials for lithium batteries with a high capacity and good cycling performance.

Max Planck Institute for Solid State Research, Heisenbergstr. 1, D-70569 Stuttgart, Germany. E-mail: Y.Hu@fkf.mpg.de; Fax: +49(0)711 6891722; Tel: +49(0)7116891725

† Electronic supplementary information (ESI) available: experimental details and electrochemical behaviour of a commercial TiO_2 electrode. See DOI: 10.1039/b605090e

Titania is one of the most intensively investigated transition metal oxides owing to its technological importance. Various nanomaterials of TiO_2 and TiO_2-based composites, such as nanoparticles, nanotubes, nanowires, nanofilms, and nanoporous solids have been synthesized and evaluated in optical devices, photovoltaic cells, catalysts, gas sensors, and electrochemical cells.[13–18] In this communication, we demonstrate that mesoporous TiO_2 can be favorably prepared from TiO_2–$CdSO_4$ composites. The advantages of the present strategy are: 1) high porosity adjustable by the volume of sacrificial compound ($CdSO_4$) in the composite; 2) larger mesopores than those prepared by soft templating methods; 3) uniform sphere size rather than uniform pore size; and 4) facility and versatility for large-scale synthesis of mesoporous structures from composite structures.

TiO_2–$CdSO_4$ were prepared by air-calcining a Ti–Cd precursor,[19] which was synthesized by mixing $Ti(OBu)_4$ with $Cd(CH_3COO)_2$ and refluxing the mixture at 140 °C for 3 hours (see Supplementary Information†). Fig. 1a shows the X-ray diffraction (XRD) pattern of the as-prepared Ti–Cd precursor, which indicates that the precursor is mainly amorphous except for a small amount of crystalline sulfur (S_6). After subsequent calcinations at 500 °C under air for 5 h, the precursor changed into TiO_2–$CdSO_4$ composite, as confirmed by the XRD pattern in Fig. 1b. It is worth noting that the environment (aerobic or anaerobic) of calcination has a marked influence on the composition of the synthesized TiO_2 composites. Under an atmosphere free of oxygen, such as N_2 and Ar, the calcined composite is TiO_2–CdS, which has been proved to be an interesting photoelectric material.[19] In order to obtain porous TiO_2 from TiO_2–$CdSO_4$, the composites are treated with dilute aqueous solution which ensures the removal of

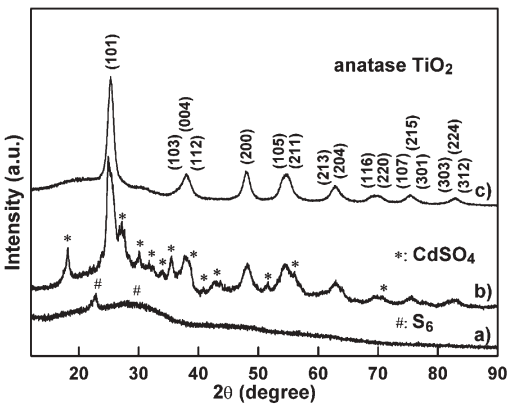

Fig. 1 X-ray diffraction patterns of a) the as-prepared Ti–Cd precursor, b) the calcinated sample, and c) the final product after the treatment with dilute HNO_3 aqueous solution.

$CdSO_4$. (The use of acid rather than water is also helpful to remove possible impurity of CdS). Fig. 1c shows the XRD pattern of the resulting sample, in which all the diffraction peaks are in good agreement with anatase TiO_2 (space group: $I4_1/amd$ (141)) with lattice constants $a = b = 3.7852$ Å and $c = 9.5139$ Å (JCPDS No. 21-1272), thus demonstrating the fabrication of pure crystalline TiO_2. The significant broadening of the diffraction peaks is ascribed to the very small size of the TiO_2 crystallites, similar to the case reported in the literature.[20] The sizes of the TiO_2 crystallites were estimated from the widths of the major diffraction peaks observed in Fig. 1c by Scherrer's formula. The mean crystallite size of D_{101} along the [101] axis is *ca.* 7 nm.

First, the morphology of the samples was investigated by scanning electron microscopy (SEM). Fig. 2a is a typical SEM image from as-prepared Ti–Cd precursor. From the image it is clear that large-scale uniform spherical particles with an average diameter of *ca.* 300 nm have been prepared. The spheres have smooth surfaces as indicated by a high magnification SEM image (the inset in Fig. 2a). After the calcining and washing, the spherical morphologies and sizes of the particles are well maintained, however, the surfaces of the spheres become significantly rough upon this removal of $CdSO_4$ and appearance of a large number of pores on the sphere surfaces is obvious from Fig. 2b and inset. Further evidence for the porous structure can be found from the high resolution transmission electron microscopy (HRTEM) image shown in Fig. 2c. Many large mesopores in size ranging from 3 nm to tens of nanometers well dispersed in the entire sphere are clearly seen in the images. Not only is the pore structure three-dimensionally interconnected, but also the spheres exhibit a three-dimensionally interconnected framework made up of nano-sized building blocks—nanoparticles—with an average size of about 7 nm, which is consistent with the above result estimated from the XRD pattern. A selected-area electron diffraction (SAED) pattern (the inset in Fig. 2c) of the sphere shows a set of concentric rings instead of sharp spots as a result of the small crystallites. The diffraction rings can be indexed to (101), (004), and (200) planes of the anatase phase (JCPDS No. 21-1272). The results demonstrate the successful preparation of mesoporous TiO_2 sub-micron spheres with the feature of three-dimensional interconnected pores and anatase nanoparticles.

In order to further examine the porous nature of the TiO_2 spheres, N_2 adsorption–desorption isotherms were employed (Fig. 3). This kind of isotherm indicates that the TiO_2 spheres belong to the mesoporous family, with the interconnected network of pores in different sizes.[21] The Barrett–Joyner–Halenda (BJH)[22] pore size distribution (the inset in Fig. 3) obtained from the

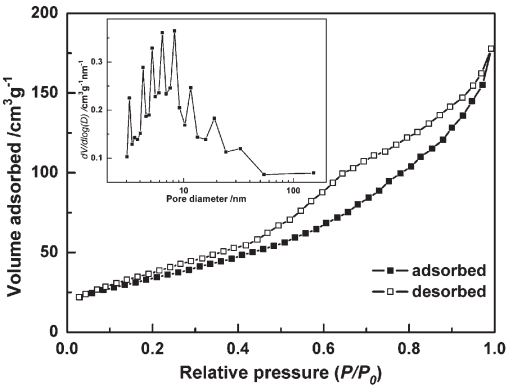

Fig. 3 Nitrogen adsorption–desorption isotherm and BJH pore size distribution plot (inset) of mesoporous TiO_2 sub-micron spheres.

isotherm indicates a number of large mesopores in various sizes of 3.2, 4.3, 5.1, 6.4, 8.3, 11.6, 19.1, and 32.9 nm exist in the sample. The average pore diameter is *ca.* 7.4 nm consistent with the HRTEM observation. The Brunauer–Emmett–Teller (BET) specific surface area of the sample was calculated from N_2 isotherms at 77.4 K, and found to be 131 m^2 g^{-1}, which totally arises from mesopores, according to our measurement. The total pore volume was 0.24 cm^3 g^{-1}. Considering the bulk density of anatase TiO_2 (1 g TiO_2 corresponds to a volume of 0.256 cm^3), the calculated porosity of the mesoporous TiO_2 spheres is 48%, which is close to the theoretical value (*ca.* 45%) obtained from the volume fraction of $CdSO_4$ in the composite. The high BET surface area and large porosity strongly support the fact that the sub-micron spheres have a mesoporous structure.

Nanostructured titania is a fast Li insertion–extraction host and also a low-voltage insertion host for Li, and hence an attractive anode material for lithium batteries.[15–18,23–25] In order to demonstrate the potential application of the present mesoporous TiO_2 sub-micron spheres, we carried out a preliminary investigation into their electroactivity for Li insertion–extraction relative to that of a commercial TiO_2 (anatase) with the same particle size. Fig. 4 shows the discharge (Li insertion)–charge (Li extraction) curves of the mesoporous TiO_2 electrode cycled in 1 M $LiPF_6$ EC/DMC (ethylene carbonate/dimethyl carbonate) electrolyte solution at a rate of C/5 (one lithium per formula unit in 5 hours). It can be seen that the first discharge curve can be divided into four regions, marked as I, II, III, IV. Correspondingly, four regions I′, II′, III′, and IV′ appear in the charging curve. For region I, it can be seen that the voltage decreases monotonically from 2.7 to 1.76 V, corresponding to a storage of 0.15 mol Li, which is a common

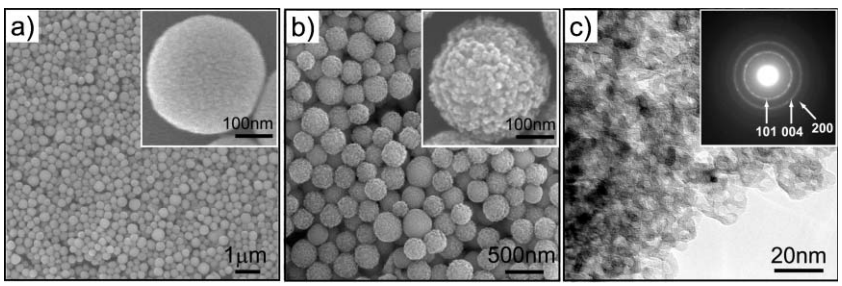

Fig. 2 a,b) SEM images of the as-prepared Ti–Cd precursor (a) and the final product (b). The insets are high-magnification SEM images showing surface structures. c) HRTEM image of part of a mesoporous TiO_2 sphere. Inset shows the corresponding SAED pattern of the sphere.

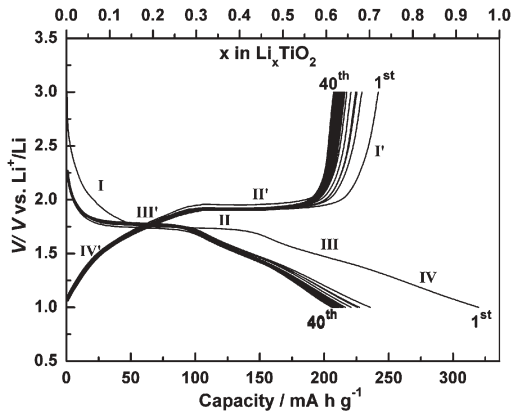

Fig. 4 Galvanostatic discharge–charge curves of mesoporous TiO_2 spheres cycled at a rate of C/5 between voltage limits of 1 and 3 V.

phenomenon linked to the decrease in particle and crystallite size for nano-sized materials.[17,25] We calculated the surface Li content per area to be 1.44×10^{-5} mol m^{-2}, similar to the case of nano-sized rutile.[25] This value is close to 3.2×10^{-5} mol m^{-2} which corresponds to the Li content of a monolayer. This indicates that the sloped region at the beginning may be due to Li surface storage of the mesoporous TiO_2.[25] The second region II (plateau) exhibits the known biphasic (Li-poor phase and Li-rich phase) process in anatase. On further Li insertion, regions III and IV with different slope appear. It is noted that the discharge voltage was usually limited above 1.3 V in other work on Li insertion into anatase TiO_2.[15,17,23,24] In our case, the discharge voltage was limited at 1 V, interestingly, it was found that these two processes (III and IV regions) are reversible (correspondingly, III′ and IV′ regions in the charge curves) during Li insertion–extraction. However, in the case of commercial TiO_2, only one process (one sloped region in the first discharge curve) was observed upon further Li insertion, and the process was not reversible (see Supplementary Information Fig. S1†). Unique properties of nano-sized materials, such as better accommodation of the structural changes during Li insertion–extraction might be indicative of the two processes.

Furthermore, the higher capacity and better cycling performance of the mesoporous TiO_2 spheres when compare to commercial TiO_2 are worth mentioning. About 0.95 mol Li can be inserted into the mesoporous TiO_2 while only 0.44 mol Li can be inserted into commercial TiO_2 in the first discharge process. Mesoporous TiO_2 spheres are able to reversibly accommodate Li up to $Li_{0.63}TiO_2$ (210 mA h g^{-1}) at 1–3 V *vs.* Li$^+$/Li with a good capacity retention on cycling (Fig. 4). The value is well comparable with that of the TiO_2–B nanowire.[18]

In conclusion, we have developed a simple method for large-scale synthesis of mesoporous uniform TiO_2 sub-micron spheres consisting of interconnected TiO_2 nanoparticles, and exhibiting large mesopores of various sizes which themselves form three-dimensional interconnected networks. In this context, it is the contribution of sub-micron size spheres and the comparatively loose packing of their nano-sized constituents that endow the material with a variety of favorable properties: The relatively large spheres enable easy operation in terms of separation or film-formation, while the comparatively large pores inside provide a network that is easily penetrated by the electrolyte. The latter, together with the nano-sized building blocks result in excellent Li insertion–extraction performance. These results suggest that the preparation of mesoporous TiO_2 sub-micron spheres leads to a promising anode material for lithium batteries. Not only is this a further example of the directed nanostructure-design for lithium batteries, but also the strategy presents a new possibility for large-scale synthesis of mesoporous structures by using composites as intermediates.

The authors would like to thank G. Götz (XRD), A. Fuchs (BET and SEM), P. Kopold (TEM) and Dr W. Sigle (HRTEM) for their technical support; Dr S. Hore and Dr W. Sigle for reading the manuscript.

Notes and references

1 M. E. Davis, *Nature*, 2002, **417**, 813.
2 S. H. Joo, S. J. Chol, I. Oh, J. Kwak, Z. Liu, O. Terasaki and R. Ryoo, *Nature*, 2001, **412**, 169.
3 C. G. Goltner, B. Smarsly, B. Berton and M. Antonietti, *Chem. Mater.*, 2001, **13**, 1617.
4 E. Kim, D. Son, T.-G. Kim, J. Cho, B. Park, K.-S. Ryu and S.-H. Chang, *Angew. Chem., Int. Ed.*, 1998, **37**, 613.
5 (*a*) C. T. Kresge, M. E. Leonowicz, W. J. Roth, J. C. Vartuli and J. S. Beck, *Nature*, 1992, **359**, 710; (*b*) D. M. Antonelli and J. Y. Ying, *Angew. Chem., Int. Ed. Engl.*, 1995, **34**, 2014.
6 (*a*) J. Ba, J. Polluex, M. Antonietti and M. Niederberger, *Adv. Mater.*, 2005, **17**, 2509; (*b*) A. S. Deshpande, N. Pinna, B. Smarsly, M. Antonietti and M. Niederberger, *Small*, 2005, **3**, 313.
7 (*a*) P. Yang, D. Zhao, D. I. Margolese, B. F. Chmelka and G. D. Stucky, *Nature*, 1998, **396**, 152; (*b*) M. Niederberger, M. H. Bartl and G. D. Stucky, *Chem. Mater.*, 2002, **14**, 4364.
8 J. Y. Ying, C. P. Mehnert and M. S. Wong, *Angew. Chem., Int. Ed.*, 1999, **38**, 56.
9 R. Ryoo, S. H. Joo, M. Kruk and M. Jaroniec, *Adv. Mater.*, 2001, **13**, 677.
10 B. Tian, X. Liu, H. Yang, S. Xie, C. Yu, B. Tu and D. Zhao, *Adv. Mater.*, 2003, **15**, 1370.
11 (*a*) J. Maier, *Nat. Mater.*, 2005, **5**, 805; (*b*) A. S. Arico, P. G. Bruce, B. Scrosati, J. M. Tarascon and W. V. Schalkwijk, *Nat. Mater.*, 2005, **4**, 366.
12 D. R. Rolison, *Science*, 2003, **299**, 1698.
13 (*a*) A. Fujishima and K. Honda, *Nature*, 1972, **238**, 37; (*b*) B. O'Regan and M. Grätzel, *Nature*, 1991, **353**, 737.
14 G. K. Boschloo, A. Goossens and J. Schoonman, *J. Electrochem. Soc.*, 1997, **144**, 1311.
15 (*a*) L. Kavan, M. Grätzel, S. E. Gilbert, C. Klemenz and H. J. Scheel, *J. Am. Chem. Soc.*, 1996, **118**, 6716; (*b*) I. Exnar, L. Kavan, S. Y. Huang and M. Grätzel, *J. Power Sources*, 1997, **68**, 720.
16 M. Wagemaker, A. P. M. Kentgens and F. M. Mulder, *Nature*, 2002, **418**, 397.
17 G. Sudant, E. Baudrin, D. Larcher and J. M. Tarascon, *J. Mater. Chem.*, 2005, **15**, 1263.
18 A. R. Armstrong, G. Armstrong, J. Canales, R. Garcia and P. G. Bruce, *Adv. Mater.*, 2005, **17**, 862.
19 J.-S. Hu, Y.-G. Guo, H.-P. Liang, L.-J. Wan and C.-L. Bai, *J. Phys. Chem. B*, 2004, **108**, 9734.
20 (*a*) J. Polleux, N. Pinna, M. Antonietti, C. Hess, U. Wild, R. Schlögl and M. Niederberger, *Chem.–Eur. J.*, 2005, **11**, 3541; (*b*) M. Niederberger, G. Garnweitner, F. Krumeich, R. Nesper, H. Cölfen and M. Antonietti, *Chem. Mater.*, 2004, **16**, 1202.
21 J. Pikunic, C. M. Lastoskie and K. E. Gubbins, in *Handbook of Porous Solids*, Vol. 1, ed. F. Schüth, K. S. W. Sing, and J. Weitkamp, Wiley-VCH, Weinheim, Germany 2002, Ch. 2.
22 E. P. Barrett, L. G. Joyner and P. P. Halenda, *J. Am. Chem. Soc.*, 1951, **73**, 373.
23 H. Yamada, T. Yamato, I. Moriguchi and T. Kudo, *Solid State Ionics*, 2004, **175**, 195.
24 L. Kavan, J. Rathousky, M. Grätzel, V. Shklover and A. Zukal, *J. Phys. Chem. B*, 2000, **104**, 12012.
25 Y.-S. Hu, L. Kienle, Y.-G. Guo and J. Maier, *Adv. Mater.*, 2006, **18**, 1421.